



Evaluation of Formability Limit Diagrams of Arsenic Brass (70/30) Using Finite Element Analysis

Author

A. Chennakesava Reddy

Professor, Department of Mechanical Engineering, JNTUH College of Engineering, Hyderabad, Telangana,
Email- chennakesava@jntuh.ac.in

ABSTRACT

Arsenic brass has high corrosion resistance against water. The aim of the present work was to establish the formability limit diagrams for Arsenic brass cylindrical cups drawn using deep drawing process. The finite element analysis software code of DEFORM-3D was used for this purpose. The process variables used in this work were temperature, strain rate, coefficient of friction and punch velocity. The reduction in the flow stress was not observed as the temperature was increased from 450°C to 600°C. The thermoplastic shear was occurred locally when the local flow stress decreased with the increase in strain rate. For higher friction constant, the necking area was moved away from the punch radius. The punch velocity has decreased the surface expansion ratio of the cylindrical cups.

Keywords- Formability limit diagram, Arsenic brass, temperature, strain rate, coefficient of friction, punch velocity

INTRODUCTION

Brass is an alloy of copper and zinc. Arsenical brass (70/30 brass) contains about 0.03% arsenic to enhance corrosion resistance in water. Arsenical brass finds applications for heat exchangers, drawn and spun containers, radiator cores, tubes, tanks, plugs, lamp fittings, locks, and cartridge casings. Deep drawing is a sheet metal forming process used for shaping flat sheets into cup-shaped articles without rupture or undue localized thinning. The process variables are the punch and die radii, the punch and die clearance, the press speed, the strain rate, the temperature, the coefficient of friction and the blank holder force. Under high strain rate conditions such as those generated in high rate metal forming, the deformation of metals and alloys is characterized by extreme strain localization along narrow shear bands [1], [2]. Furthermore, a decrease in grain size, for a given rate of deformation, results in a decrease in flow stress [3]. For conventional polycrystalline metals, the temperature must be above $0.5 T_m$ (where T_m is the absolute melting temperature of the material) so that very high

elongation in tension can be achieved without any significant necking [4].

Sheet metal formability is often evaluated by forming limit diagram. The concept of formability limit diagrams was first introduced by Keeler [5] and Goodwin [6]. The formability limit diagrams are established for several materials such as AA1050 [7], AA 2008 [8], AA2014 [9], AA2017 [10], AA2024 [11], AA2219 [12], AA2618 [13], AA3003 [14], AA5049 [15], AA5052 [16], AA5556 [17] and AA6061 [18], [19].

The objective of the present work was to establish the formability limit diagram for the arsenical brass for fabrication of cylindrical cups. The deep drawing process was modelled using finite element analysis software. The numerical results were validated with the experimental results.

FINITE ELEMENT MODELLING

The finite element modeling and analysis was carried using D-FORM 3D software. The cylindrical sheet blank was created with desired diameter and thickness using CAD tools. The cylindrical top punch, cylindrical bottom hollow die

were also modeled with appropriate inner and outer radius and corner radius using CAD tools. The clearance between the punch and die was calculated as in Eq. (1). The sheet blank was meshed with tetrahedral elements.

$$\text{Clearance, } c = t \pm \mu\sqrt{10t} \quad (1)$$

In the present work, moving blank die was used to hold the blank at a predefined speed different to the punch speed. The contact between blank/punch and die/blank were coupled as contact pair. The mechanical interaction between the contact surfaces was assumed to be frictional contact and modeled as Coulomb's friction model as defined in Eq. (3). The finite element analysis was chosen to find the metal flow, effective stress, height of the cup, and damage of the cup. The finite element analysis was carried out using D-FORM 3D software according to the design of experiments. The Coulomb's friction model was given by

$$\tau_f = \mu p \quad (2)$$

RESULTS AND DISCUSSION

The dimensions of cylindrical cups drawn in the present work were 60 mm diameter and 75 mm height. The process variables were temperature, strain rate, coefficient of friction, and punch velocity. The blank holder was movable type and it was moved at constant velocity 0.4 mm/s irrespective of the said process variables. While studying one process variable the rest of them were maintained univariable.

3.1 Effect of Process Variables on von Mises Stress

The general trend of decreasing of von Mises stress with increasing temperature is observed as shown in Fig. 1. This trend confirms with the results obtained from the tensile test experimentally as shown in Fig. 2. In general, the reduction in the flow stress with increasing temperature confirms that the alloy is temperature sensitive. Although there is no obvious reduction in the flow stress as the temperature is increased from 450°C to 600°C. As observed from Fig. 2 the ductility increases with increase in temperature. This confirms with surface expansion ratios as shown in Fig. 3. The values of strain rate,

coefficient of friction, and punch velocity were, respectively, 100.0 s⁻¹, 0.25 and 2.0 m/s.

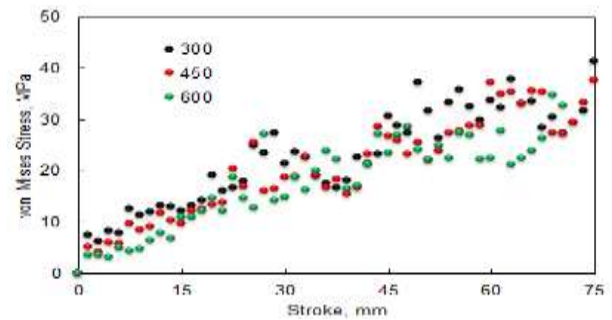


Fig. 1 Effect of temperature on von Mises stress.

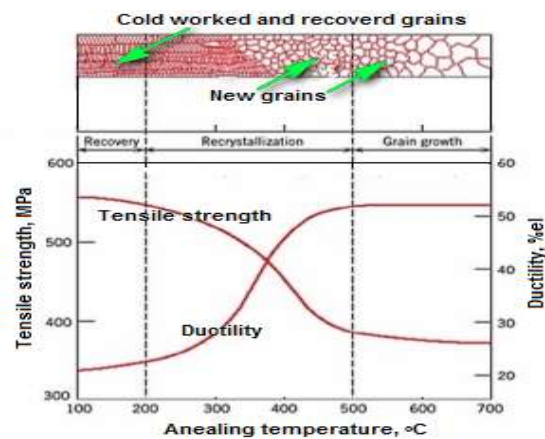


Fig. 2 Effect of annealing temperature on tensile strength and ductility.

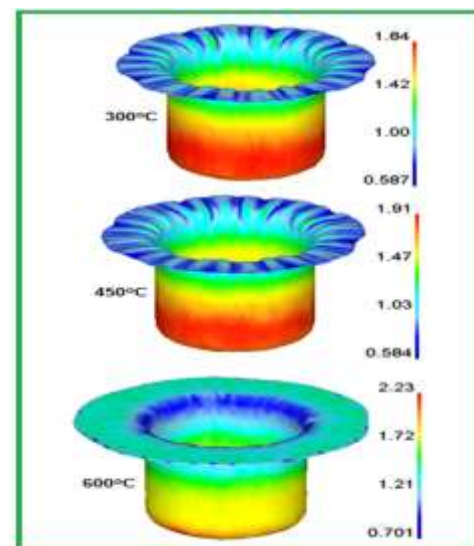


Fig. 3 Effect of temperature on surface expansion ratio.

Very interestingly, the von Mises stress decreases with increase in the strain rate as seen from Figs. 4 and 5. For effect of strain rate on von Mises stress, the other process variables such as temperature, coefficient of friction, and punch velocity were

maintained at constant values of 450°C, 0.25 and 2.0 m/s, respectively. This phenomenon may occur when the rate of thermal softening due to the internally generated heat exceeds the rate of isothermal work hardening during deep drawing process. The thermoplastic shear occurs locally when the local flow stress decreases with the increase in strain rate.

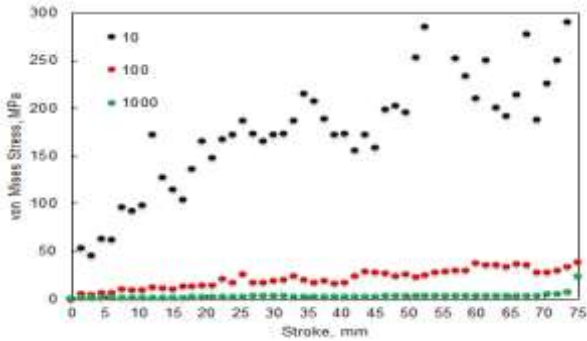


Fig. 4 Effect of strain rate on von Mises stress.

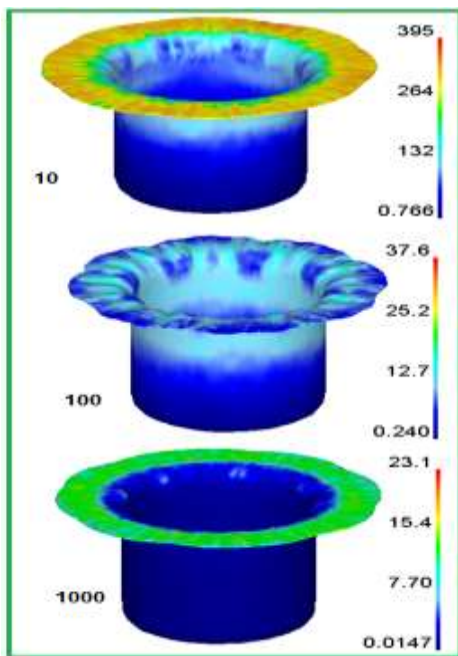


Fig. 5 Effect of strain rate on von Mises stress.

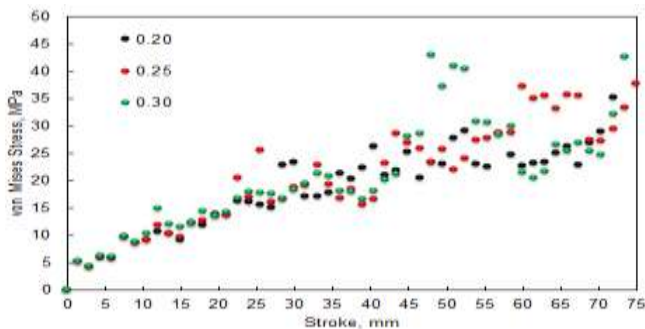


Fig. 6 Effect of friction coefficient on von Mises stress.

The von Mises stress is not influenced by the variation of coefficient of friction as shown in Fig. 6. But, the punch velocity affects the von Mises stress as shown in Fig. 7. The von Mises stress increases with increase in the punch velocity.

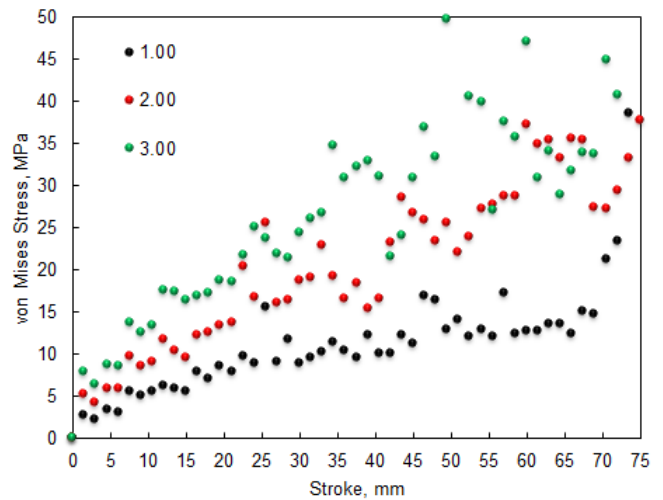


Fig. 7 Effect of punch velocity on von Mises stress.

3.2 Effect of Process Variables on Formability

Effect of temperature on the formability of brass cups is shown in Fig. 8. Below 450°C, the formation of wrinkles is noticed in the flange area of cups as seen from Fig. 3. The surface expansion ratio is sufficiently high to avoid the formation of wrinkles in the brass cups at 600°C. At 600°C, the deep drawing process is dominated shear phenomena only. At 300°C and 450°C the sheet material has experienced either compression or uni-axial tension during deep drawing of the cups.

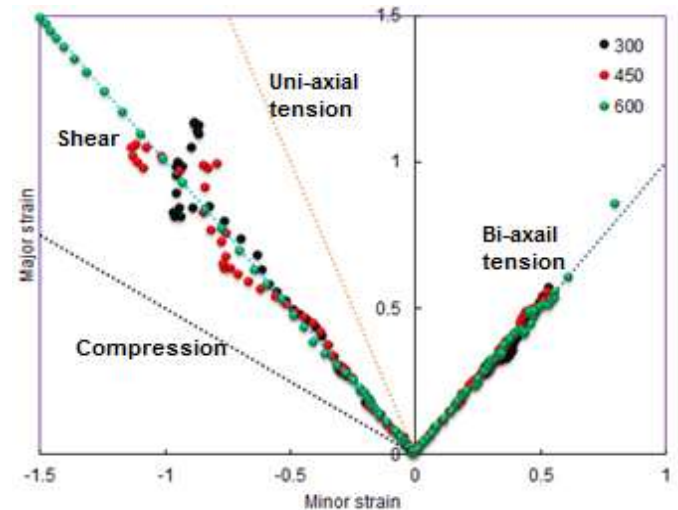


Fig. 8 Effect of temperature on formability of brass cups.

Effect of strain rate on the formability of brass cups is shown in Fig. 9. The surface expansion ratio is, respectively, 2.01, 1.84 and 2.26 for strain rates 10, 100, and 1000.

100 and 1000 s^{-1} . The difference between the strain rates is to limit the reliability band of the forming limit diagram over the shear line also known as deep drawing line. Also, it is observed that at a given temperature, the arsenic brass becomes increasingly sensitive to the strain rate at higher values of the strain. At three strain rates the wrinkles are formed in the flange area of brass cups as seen in Fig. 10. At three strain rates the sheet material has undergone compression and tension over the strain of 0.3. The formation of wrinkles is due to compressive stresses in the plane of the sheet material.

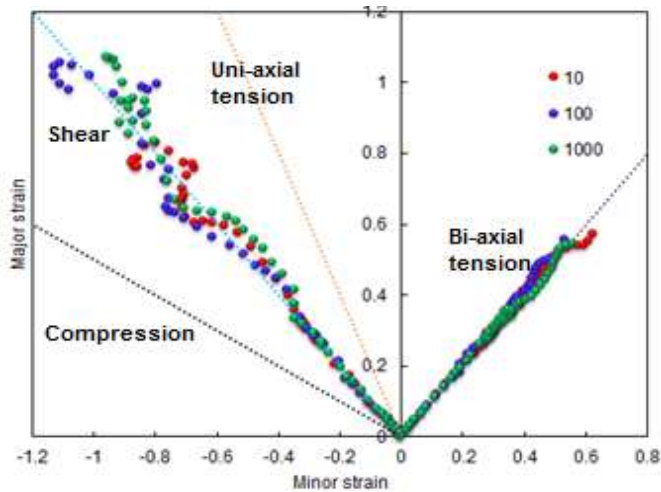


Fig. 9 Effect of strain rate on formability of brass cups.

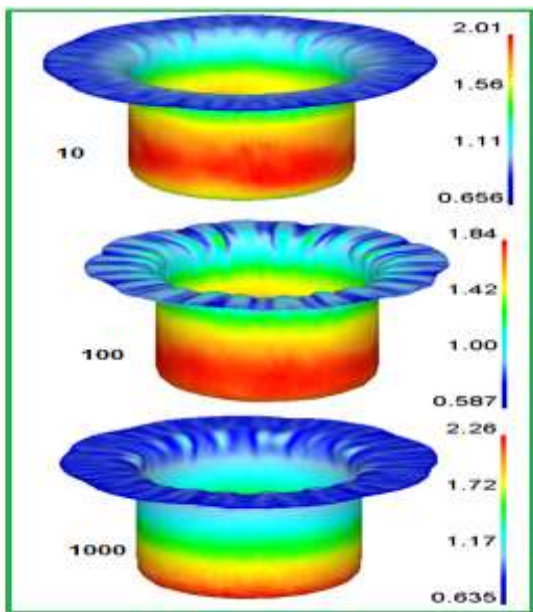


Fig. 10 Effect of strain rate on surface expansion ratio.

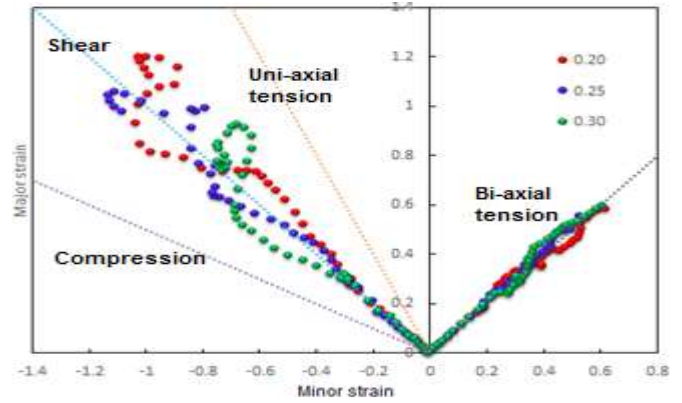


Fig.11 Effect of friction coefficient on formability of cups.

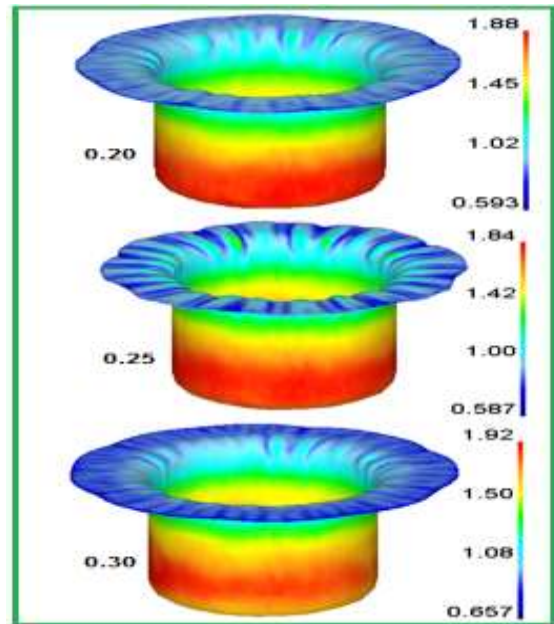


Fig. 12 Effect of friction coefficient on surface expansion ratio.

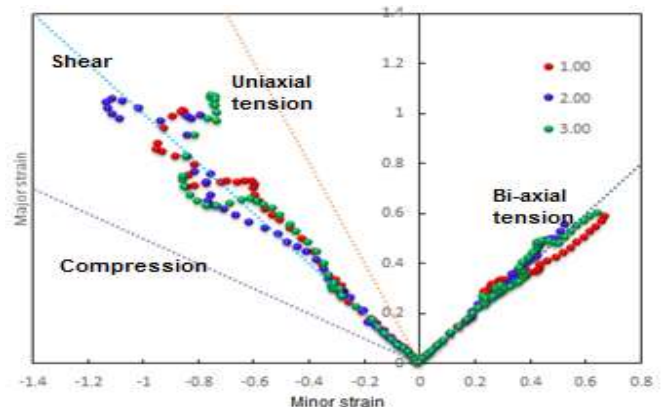


Fig.13 Effect of punch velocity on formability of cups.

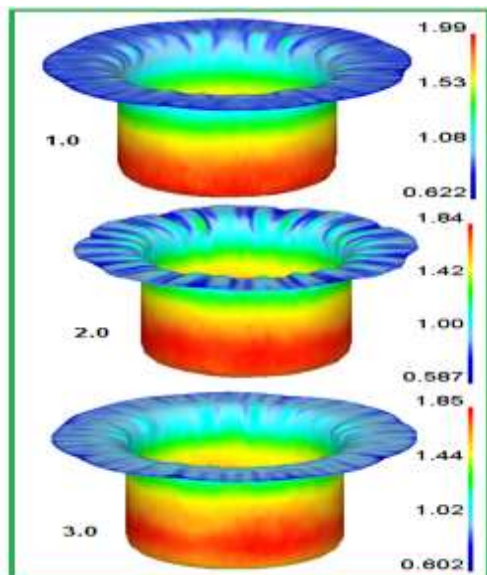


Fig.14 Effect of punch velocity on surface expansion ratio.

The effect of friction coefficient on the formability of brass cups is shown in Fig. 11. The surface expansion ratio is, respectively, 1.88, 1.84 and 1.92 for friction coefficients of 0.20, 0.25 and 0.30 as shown in Fig. 12. The formability curves are either side of pure shear line resulting the formation of wrinkles in the brass cups. The obtained results show that at lower coefficient of friction constants the necking area is closer to the punch radius as in the case when $\mu = 0.20$ and 0.25 . For higher friction constant, at $\mu = 0.30$, the necking area moves away from the punch radius. Biaxial tension is accompanied by thinning and typically occurs in spherical shapes such as at the punch nose [20]. Therefore, in a real deep drawing process and finite element analysis, the choice of friction coefficient is highly influential on the deformations on the sheet. The effect of punch velocity on the formability of brass cups is shown in Fig. 13. As the punch velocity increases the surface expansion ratio decreases imparting less time to expand the sheet material as shown in Fig.14. At three punch velocities, the wrinkles are seen in the brass cups.

CONCLUSIONS

The finite element modelling and analysis could effectively predict the formability limit diagrams for arsenic brass. The formability limit curves of cylindrical cups were spread around the shear line of the arsenic brass. The arsenic brass was sensitive

to temperature above 450°C . The range of strain rates between 10 s^{-1} to 1000 s^{-1} could limit the reliability band of the forming limit diagram over the shear line. The high coefficient of friction, at $\mu = 0.30$, the necking of sheet material was moved away from the punch radius.

Acknowledgement

The author thanks University Grants Commission (UGC), New Delhi for financial assisting this project work.

REFERENCES

1. K. Wang, "The Use and Properties of Titanium and Titanium Alloys for Medical Applications in the USA," Materials Science and Engineering, vol. A213, pp. 134–137, 1996.
2. P. S. Follansbee: Metals Handbook. Mechanical Testing, J. R. Newby (Ed.), vol. 8, 9th edition, ASM, Ohio, pp. 190–192, 1985.
3. T. G. Nieh, J. Wadsworth, O. D. Sherby, "Superplasticity in Metals and Ceramics," Cambridge University Press, New York, 1997.
4. T. G. Langdon, "The mechanical properties of superplastic materials," Metallurgical Materials Transactions A vol. 13A, pp. 689–701, 1982.
5. S. P. Keeler, "Determination of forming limits in automotive stampings," SAE Technical Paper, vol. 42, pp. 683–691, 1965.
6. G. M. Goodwin, "Application of strain analysis to sheet metal forming problems in the press shop," SAE Technical Paper, 60, pp. 764–774, 1968.
7. A. C. Reddy, "Performance of Warm Deep Drawing Process for AA1050 Cylindrical Cups with and Without Blank Holding Force," International Journal of Scientific Research, vol. 4, no. 10, pp. 358–365, 2015.
8. Graf, W. Hosford, Effect of changing strain paths on forming limit diagrams of Al 2008-T4," Metallurgical Transactions A, vol. 24, pp. 2503–2512, 1993.

9. C. Reddy, "Parametric Optimization of Warm Deep Drawing Process of 2014T6 Aluminum Alloy Using FEA," International Journal of Scientific & Engineering Research, vol. 6, no. 5, pp. 1016-1024, 2015.
10. C. Reddy, "Finite Element Analysis of Warm Deep Drawing Process for 2017T4 Aluminum Alloy: Parametric Significance Using Taguchi Technique," International Journal of Advanced Research, vol. 3, no. 5, pp. 1247-1255, 2015.
11. C. Reddy, "Parametric Significance of Warm Drawing Process for 2024T4 Aluminum Alloy through FEA," International Journal of Science and Research, vol. 4, no. 5, pp. 2345-2351, 2015.
12. C. Reddy, "Formability of High Temperature and High Strain Rate Superplastic Deep Drawing Process for AA2219 Cylindrical Cups," International Journal of Advanced Research, vol. 3, no. 10, pp. 1016-1024, 2015.
13. R. Alavala, "High temperature and high strain rate superplastic deep drawing process for AA2618 alloy cylindrical cups," International Journal of Scientific Engineering and Applied Science, vol. 2, no. 2, pp. 35-41, 2016.
14. R. Alavala, "Practicability of High Temperature and High Strain Rate Superplastic Deep Drawing Process for AA3003 Alloy Cylindrical Cups," International Journal of Engineering Inventions, vol. 5, no. 3, pp. 16-23, 2016.
15. R. Alavala, "High temperature and high strain rate superplastic deep drawing process for AA5049 alloy cylindrical cups," International Journal of Engineering Sciences & Research Technology, vol. 5, no. 2, pp. 261-268, 2016.
16. R. Alavala, "Suitability of High Temperature and High Strain Rate Superplastic Deep Drawing Process for AA5052 Alloy," International Journal of Engineering and Advanced Research Technology, vol. 2, no. 3, pp. 11-14, 2016.
17. R. Alavala, "Development of High Temperature and High Strain Rate Super Plastic Deep Drawing Process for 5656 Al Alloy Cylindrical Cups," International Journal of Mechanical and Production Engineering, vol. 4, no. 10, pp. 187-193, 2016.
18. R. Alavala, "Effect of Temperature, Strain Rate and Coefficient of Friction on Deep Drawing Process of 6061 Aluminum Alloy," International Journal of Mechanical Engineering, vol. 5, no. 6, pp. 11-24, 2016.
19. Djavanroodi, A. Derogar, "Experimental and numerical evaluation of forming limit diagram for Ti6Al4V titanium and Al6061-T6 aluminum alloys sheets," Journal of Materials & Design, vol. 3, pp. 4866-4875, 2010.
20. C. Reddy, "Evaluation of local thinning during cup drawing of gas cylinder steel using isotropic criteria," International Journal of Engineering and Materials Sciences, vol. 5, no. 2, pp. 71-76, 2012.